The Astrophysical Journal Letters, 872:L19 (8pp), 2019 February 20 https://doi.org/10.3847/2041-8213/ab03d6

The Spectral Properties of the Bright Fast Radio Burst Population

J.-P. Macquart[1,2], R. M. Shannon[3], K. W. Bannister[4], C. W. James[1], R. D. Ekers[1,4], and J. D. Bunton[4]
[1] International Centre for Radio Astronomy Research, Curtin University, Bentley, WA 6102, Australia; J.Macquart@curtin.edu.au
[2] ARC Centre of Excellence for All-sky Astrophysics (CAASTRO), Australia
[3] Centre for Astrophysics and Supercomputing, Swinburne University of Technology, P.O. Box 218, Hawthorn, VIC 3122, Australia
[4] Australia Telescope National Facility, CSIRO Astronomy and Space Science, P.O. Box 76, Epping, NSW 1710, Australia
Received 2018 September 26; revised 2019 January 15; accepted 2019 January 30; published 2019 February 14

Abstract

We examine the spectra of 23 fast radio bursts (FRBs) detected in a fly's-eye survey with the Australian SKA Pathfinder, including those of three bursts not previously reported. The mean spectral index of $\alpha = -1.5^{+0.2}_{-0.3}$ ($F_\nu \propto \nu^\alpha$) is close to that of the Galactic pulsar population. The sample is dominated by bursts exhibiting a large degree of spectral modulation: 17 exhibit fine-scale spectral modulation with an rms exceeding 50% of the mean, with decorrelation bandwidths (half-maximum) ranging from ≈1 to 49 MHz. Most decorrelation bandwidths are an order of magnitude lower than the ≳30 MHz expected of Galactic interstellar scintillation at the Galactic latitude of the survey, $|b| = 50° \pm 5°$. However, these bandwidths are consistent with the $\sim\nu^4$ scaling expected of diffractive scintillation when compared against the spectral structure observed in bright UTMOST FRBs detected at 843 MHz. A test of the amplitude distribution of the spectral fluctuations reveals only 12 bursts consistent at better than a 5% confidence level with the prediction of 100%-modulated diffractive scintillation. Five of six FRBs with a signal-to-noise ratio exceeding 20 are only consistent with this prediction at less than 1% confidence. Nonetheless, there is weak evidence (92%–94% confidence) of an anti-correlation between the amplitude of the spectral modulation and dispersion measure (DM), which suggests that it originates as a propagation effect. This effect is corroborated by the smoothness of the higher-DM Parkes FRBs, and could arise due to quenching of diffractive scintillation (e.g., in the interstellar medium of the host galaxy) by angular broadening in the intergalactic medium.

Key words: radiation mechanisms: non-thermal – surveys

1. Introduction

The extreme brightness of the radiation observed from fast radio bursts (FRBs) requires that it is generated by a coherent emission process. The millisecond durations of FRB events and their inferred cosmological distances (Lorimer et al. 2007; Tendulkar et al. 2017) together imply that their brightness temperatures exceed 10^{35} K, surpassing those of most radio pulsars, whose emission has long been recognized to inescapably involve generation by a coherent process (see Melrose & Yuen 2016, for a recent review). A yet more acute problem is posed by the luminosity: the 1–800 Jy flux density emission observed in the bright FRB population, if generated at cosmological distances, is inferred to be over 12 orders of magnitude more luminous than the brightest Galactic pulsars. Moreover, the 1–390 Jy ms fluences imply energies in excess of $\sim 10^{34}(\Omega_b/4\pi)$J for a beam solid angle Ω_b even if the emission is only confined to the observational bandwidth of ≈300 MHz (Bannister et al. 2017).

The origin of such luminous emission is a matter of conjecture (e.g., Vachaspati 2008; Cordes & Wasserman 2016; Metzger et al. 2017). As such, the spectrum of the emission is both fundamental to characterizing the emission process and to quantifying the total radio energy output. Furthermore, fine-scale spectral structure, at ∼10 MHz and finer scales, is detected in some FRBs (Ravi et al. 2016; Farah et al. 2018; Oslowski et al. 2018) and is even time-variable in the one repeating FRB 121102 (Spitler et al. 2016).

The spectral properties of the FRB population have hitherto been unclear due to the manner in which most of these events have been detected. The 64 m Parkes radio telescope, responsible for the plurality of FRB detections to date (Petroff et al. 2016), uses a 13-beam multibeam receiver whose large separation between adjacent beams renders each burst location sufficiently uncertain; as a consequence, beam chromaticity effects insert substantial, generally indeterminable large-scale structure in the shape of the observed spectrum. Indeed, this is the case for all telescopes that do not adequately sample the focal plane. By contrast, the phased-array feeds (PAFs) of the Australian SKA Pathfinder (ASKAP; McConnell et al. 2016) fully sample the focal plane and thus enable each burst to be localized sufficiently well to eliminate the effects of beam chromaticity.

Shannon et al. (2018) presented the discovery of 20 FRBs in a fly's eye survey conducted at a Galactic latitude of $|b| = 50° \pm 5°$ under the auspices of the Commensal Real-time ASKAP Fast Transients (CRAFT; Macquart et al. 2010) survey on ASKAP. Here we examine spectral properties of this bright FRB population. In Section 2, we augment the sample with three additional FRB detections. In Section 3 we analyze the fluence spectra of these 23 ASKAP-CRAFT FRBs. In Section 4 we examine several possible interpretations of their remarkable spectral structure, and in Section 5 we discuss the wider implications of our results.

2. Recent FRB Searches

The analysis presented here is based on the CRAFT observations reported in Bannister et al. (2017), with further details in Shannon et al. (2018). Since the conclusion of those searches we have undertaken a few small additional surveys. Searches were conducted in the same observing band, centered at 1320 MHz, with a total of 336 MHz of bandwidth, subdivided into samples of 1 MHz width and 1.26 ms duration. Burst properties were measured from the data using the

techniques presented in Bannister et al. (2017) and Shannon et al. (2018).

Here we present the discovery of three additional FRBs in this period. The properties of the FRBs are listed in Table 1 and the profiles and spectra are shown in Figure 1.

Two FRBs (180315 and 180424) were discovered in a survey conducted at a Galactic latitude of $|b| = 20°$. The Galactic dispersion measure (DM) contribution to the bursts (DM_{MW}, see Table 1), the sum of a Galactic disk and halo component, is higher than that of the $b = 50°$ FRBs, but still much smaller than the total burst DM. For the disk component, we have assumed the NE2001 electron density model Cordes & Lazio (2002). The halo component is estimated to be 15 pc cm^{-3} from the DM excess in the direction the Large Magellanic Cloud pulsars, as elaborated in Shannon et al. (2018). However, we note that there is considerable variation in the estimated halo contribution (see, e.g., Dolag et al. 2015). The $|b| = 20°$ searches comprised 71 antenna-days. Assuming a survey-equivalent effective field of view of 20 deg^2, and 80% observing efficiency (Shannon et al. 2018) this is a rate of one FRB per 13,600 deg^2 hr exposure, or 72 sky^{-1} day^{-1}. Both show spectral modulation similar to that observed in the sample presented in Shannon et al. (2018). The third burst, FRB 180525, was detected in further high Galactic latitude ($b = 50°$) searches.

As our searches frequently re-observed the same fields, we can place strong constraints on repetition for these three bursts. The last column of Table 1 lists the amount of time spent observing these fields for repeat bursts. More than 22 days has been observed in the direction of FRB 180525.

3. Observations and Spectral Properties

The spectra reported here were corrected for the variation in T_{sys} across the observing band in the same manner reported in Shannon et al. (2018). The close spacing of beams within the ASKAP PAFs enables each burst to be localized to within a small fraction of the beamwidth, typically within a region that is $10' \times 10'$. The spectrum and fluence of each burst were corrected for the small off-axis beam chromaticity using the fact that, for the small offsets from beam center relevant to these FRBs, the beam is well approximated as a Gaussian with a full-width at half power of 1.05 $(\lambda/0.2\,\mathrm{m})$ deg, for the $D = 12$ m dish diameter (McConnell et al. 2016); details of this typically ∼1%–5% correction are discussed in Bannister et al. (2017) and Shannon et al. (2018). Both FRB 171216 and FRB 180525 were detected with comparable signal-to-noise ratio (S/N) in two beams, with offsets of 0.°491 and 0.°43, and 0.°5 and 0.°513, respectively, from the beam center. We applied the beam correction to the spectrum of each beam separately before computing the weighted average spectrum of the data from the two beams.

3.1. Broadband Spectrum

Figure 2 shows the mean and median spectrum of the 23 FRBs in our sample, with each burst given equal weight in the average by normalizing by its mean fluence. A strong trend of decreasing fluence with frequency is visible over the 336 MHz observing band, which we characterize by fitting a power law of the form $F_\nu \propto \nu^\alpha$. The spectral index of the mean spectrum is $\alpha = -1.5^{+0.2}_{-0.3}$, while for the median spectrum it is $\alpha = -1.3^{+0.4}_{-0.2}$. These values are within 1 standard deviation of the results reported in Shannon et al. (2018) on the basis of the first 20 FRBs detected in the CRAFT survey.

Table 2 lists the spectral indices obtained from the fits to individual spectra (where the errors from the fits are typically $\ll 1$ and at most still <1). The median spectral index is $\alpha = -1.1$ and the standard deviation is 4. The distribution of individual burst spectral indices shown in Figure 3 demonstrates that the distribution of the spectral index has a clear peak. The large variation in α is in part a reflection of the patchiness of the emission. For instance, for FRBs 170906 and 171019 the spectrum is entirely dominated by emission in the lower half of the band, whereas for FRB 180128.2 the spectrum is dominated by the upper half of the band. We note that the error from fitting the mean spectrum is significantly lower than the standard error of the mean of the distribution of individual spectral indices. This is because the average of the mean spectrum uses all of the information in each spectrum, and is not the equivalent to an average over individual spectral indices.

3.2. Characterization of Spectral Variations

A significant subset of the CRAFT bursts exhibit large-amplitude narrowband spectral variability.The amplitude of the variability is characterized using the square of the modulation index, m^2. This is calculated using two methods: (i) computing the mean-normalized spectral autocovariance directly from the spectrum, $f(\Delta\nu) = \langle [F_\nu(\nu' + \Delta\nu) - \bar{F}_\nu][F_\nu(\nu') - \bar{F}_\nu]\rangle / \bar{F}_\nu{}^2$, and (ii) identical to (i), except with $\bar{F}_\nu$ replaced by the best-fitting function of the form $K\nu^{-1.5}$ whose value K is chosen to preserve the band-average fluence of the burst. The values of m^2 and $m^2_{\alpha,\mathrm{corr}}$ so obtained from methods (i) and (ii), respectively, are determined by examining the value of f at spectral lags close to zero, but not identically at zero lag, which contains the additional unwanted contribution due to the noise variance. (To be clear, the value of $m_{\alpha,\mathrm{corr}}$ is defined as the modulation index of the intensity variations after subtraction of a mean spectrum of spectral index -1.5 and normalization of the intensity variations across the band by the same spectral index. Where the mean spectrum is known, this is formally the correct estimator of the spectral modulations, whereas the approximation of method (i) is more robust.) In both cases, the decorrelation bandwidth, ν_{dc}, is calculated as the half-width at half-power value of $f(\Delta\nu)$, i.e., the smallest value of $\Delta\nu$ at which $f(\Delta\nu)$ falls below $0.5f(0)$. Both methods were further checked for consistency against a robust estimate of the variance by subtracting in quadrature the variance due to the thermal noise, measured from the off-pulse spectrum, from the total spectral variance. The 32/27 oversampling of the 1 MHz coarse spectral channels on ASKAP results in at most a correction of 1% to the values of m^2 that we report here.

A possible cause of this narrowband structure is diffractive scintillation, which makes a clear prediction for the statistics of the intensity fluctuations. The amplitude distribution of a point source subject to diffractive scintillation is an exponential (Mercier 1962; Salpeter 1967) which, when convolved with normally distributed[5] noise, $\mathcal{N}(I)$ with variance σ_t, predicts

[5] In the present case, noise in the dynamic spectrum is expected to follow a χ^2 distribution with >3000 degrees of freedom, which is excellently approximated by a normal distribution.

Table 1
Properties of the Newly Discovered FRBs

FRB	Time (TAI)[a]	DM (pc cm^{-3})	F_ν (Jy ms)	R.A. (J2000) (hh:mm)[b]	Decl. (J2000) (dd:mm)[b]	g_l (deg.)	g_b (deg.)	w (ms)	Signal-to-noise Ratio (S/N)[c]	$\mathrm{DM_{MW}}$[d] (pc cm^{-3})	$\mathrm{DM_{EG}}$ (pc cm^{-3})	T_{obs} (d)
180315	05:06:07.9851(2)	479.0(4)	56(4)	19:35(3)	−26:50(10)	13.2	−20.9	2.4(3)	10.4	116	363	2.5
180324	09:32:23.7066(3)	431.0(4)	71(3)	06:16(3)	−34:47(10)	245.2	−20.5	4.3(5)	9.8	79	352	2.0
180525	15:19:43.51508(3)	388.1(3)	300(6)	14:40(2)	−02:12(6)	349.0	50.7	3.8(1)	27.4	46	303	21.6

Notes.
[a] Arrival times refer to TAI (not UTC) and are referenced to a frequency of 1297 MHz.
[b] Uncertainties are the marginalized 90% containment regions.
[c] S/N as reported in the search.
[d] The Milky Way dispersion measure (DM; $\mathrm{DM_{MW}}$) contribution is the sum of a disk (Cordes & Lazio 2002) and halo DM components; the extra-Galactic DM component ($\mathrm{DM_{EG}}$) is the difference between the two.

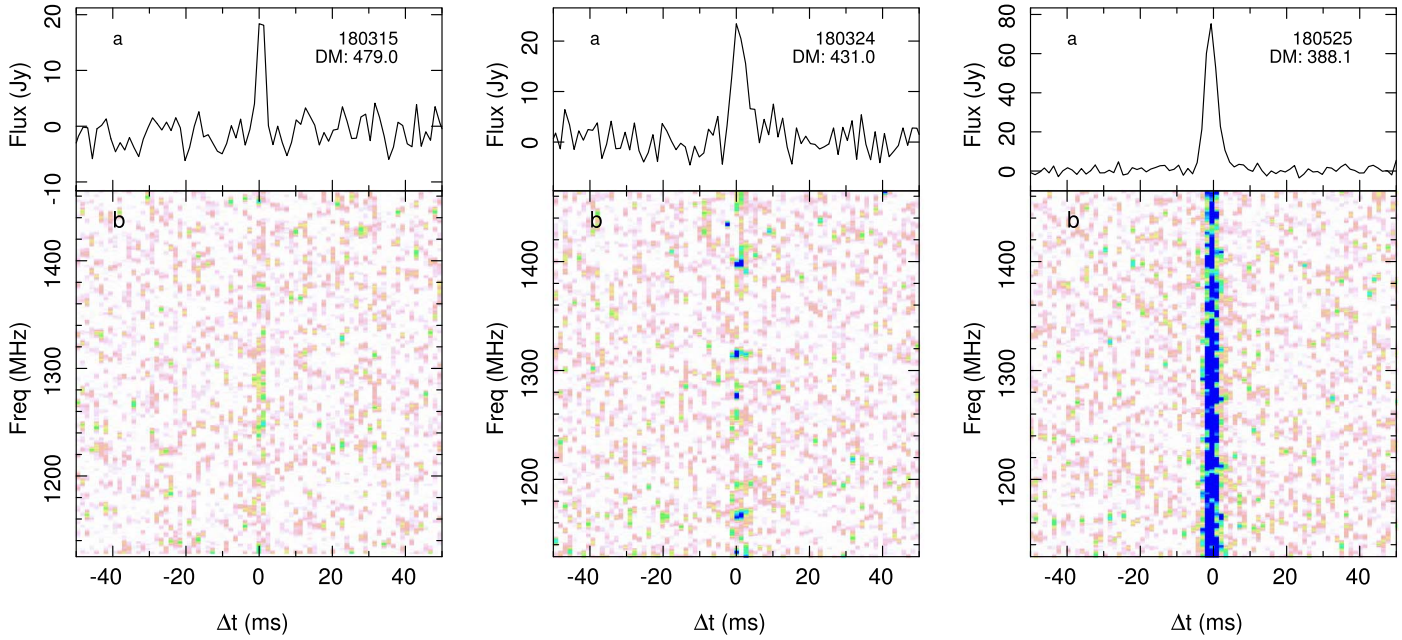

Figure 1. Pulse profiles (panels A) and dynamic spectra (panels B) of newly reported FRBs. As in Shannon et al. (2018), the color scale is set to saturate at 5σ, where σ is the off-pulse rms.

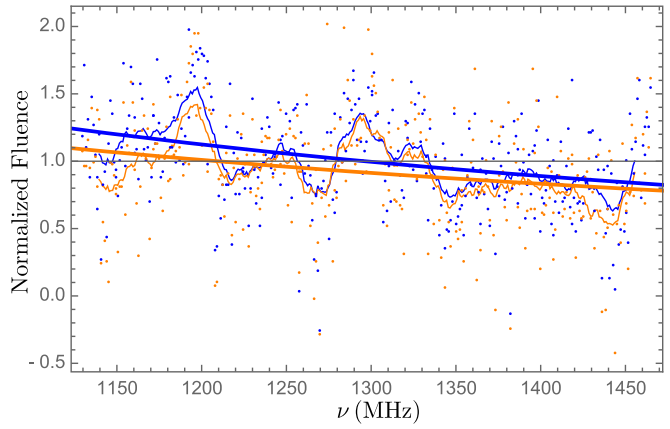

Figure 2. Equal-weight average flux density spectrum from the set of 23 ASKAP-CRAFT FRBs. Blue and orange points indicate, respectively, the mean and median fluence of each spectral channel, the light blue and orange curves indicate the 20 MHz unweighted moving average of the mean and median fluence, and the heavy lines indicate the corresponding best-fit (least-squares) power-law curves to the spectral channel data.

spectral fluctuations of the form

$$p_I(I) = \int_0^\infty \frac{1}{I_0}\exp\left(-\frac{I'}{I_0}\right)\mathcal{N}(I-I')dI' = \frac{1}{2I_0}\exp\left(\frac{\sigma_t^2}{2I_0^2}-\frac{I}{I_0}\right)\mathrm{erfc}\left[\frac{1}{\sqrt{2}}\left(\frac{\sigma_t}{I_0}-\frac{I}{\sigma_t}\right)\right], \quad (1)$$

where erfc is the complementary error function, and I_0 is the mean flux density. Because the scintillation signal is highly correlated over a spectral range $\approx\nu_{\rm dc}$, we test this distribution against the statistics of each spectrum binned to a resolution of $\lceil\nu_{\rm dc}/1\ \mathrm{MHz}\rceil$. The rms noise, σ_t, is measured directly from off-pulse data adjacent to the burst arrival time, and scaled according to the number of 1 MHz spectral bins averaged together.

Table 2 shows the confidence, using the Cramér–von Mises test, that the spectral data matches the model in Equation (1). The test is performed by (i) comparing the distribution of channelized fluences directly against the distribution, or (ii) using the channelized fluences normalized by the power law whose spectral index matches that of the median burst spectrum (i.e., $\alpha=-1.5$) and whose band-averaged fluence matches that of the burst.

Twelve bursts have intensity distributions that are consistent with the distribution of Equation (1) at the 5% confidence level or greater. Figure 4 shows the observed and predicted distributions for the six brightest bursts. Five of these six FRBs with an S/N greater than 20 are inconsistent with the predicted distribution (i.e., the observed data have less than a 1% confidence of being consistent with the model). The exception, FRB 171019, has $\nu_{\rm dc}=49$ MHz, and hence the test, is weakened by having only seven effective samples across the band.

4. Interpretation

The most significant feature of the bright burst spectra observed by ASKAP is the high degree of spectral modulation. It is an open question whether or not these are characteristic of the burst emission process or of a propagation effect. The former is expected on the grounds that many coherent emission processes (e.g., Jovian decametric radiation, solar radio bursts and, notably, even giant pulses from the Crab pulsar) exhibit fine spectral structure, many of which may persist in time (Ellis 1969; Hankins & Eilek 2007; Melrose 2017, and references therein). However, the millisecond duration of FRBs indicates that they are sufficiently compact that their spectra should also be subject to lensing and diffractive scintillation effects caused by inhomogeneous plasma in our Galaxy, the host galaxy, or possibly the intergalactic medium (IGM).

The spectral structure might be associated with caustics due to plasma lensing, as suggested by Cordes et al. (2017). If

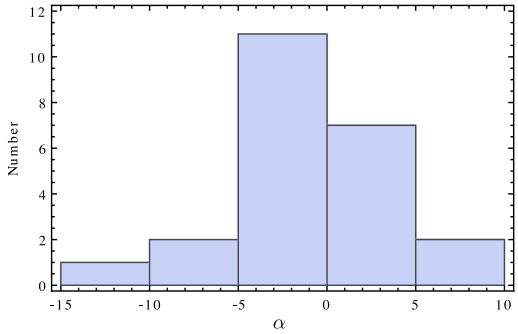

Figure 3. Distribution of individual burst spectral indices α ($F_\nu \propto \nu^\alpha$).

attributable to caustics, the interpretation is complicated by the high degree of spectral structure evident in many of the bursts. A large number of bright islands of power are evident in most spectra (the clearest examples being FRBs 170416, 171019, 180110, and 180324). These spectra do not qualitatively resemble those of other astrophysical events recognized to be associated with caustics, notably extreme scattering events (e.g., Bannister et al. 2016). The high degree of spectral structure would in turn require a high degree of structure in the lensing medium (e.g., clumps, or possibly even gaps in the plasma density).

The narrowband nature of diffractive scintillation provides a natural interpretation of the observed spectral structure. Circumstantial support of the diffractive scintillation interpretation is provided by observations of FRBs at slightly lower frequencies: the bandwidth of the spectral structure is consistent with the scaling that one would expect for diffractive scintillation between 843 MHz and 1.4 GHz. Spectral structure is clearly evident in two UTMOST FRBs whose high flux densities and a recently implemented voltage capture system facilitate a detailed analysis of fine spectral structure. FRB 170827 shows spectral modulation on scales of both 0.1 and 1.5 MHz at 843 MHz (Farah et al. 2018) implying, respectively, $\nu_{\rm dc} \approx 0.8$ and 11 MHz at 1.4 GHz for a $\nu_{\rm dc} \propto \nu^{-4}$ scaling. FRB 181017 exhibits strong modulations on a scale of 0.5 MHz (W. Farah et al. 2019, in preparation) implying $\nu_{\rm dc} = 4$ MHz at 1.4 GHz. Thus there is broad consistency between the bandwidth of the structure at the two frequencies if interpreted in terms of diffractive scintillation.

However, for the high Galactic latitude ($|b| \approx 50°$) FRBs reported here, the decorrelation bandwidth expected due to Galactic interstellar scintillation is ~20–200 MHz (Cordes & Lazio 2002; Bhat et al. 2018); all but three bursts in the sample exhibit decorrelation bandwidths that are less than 20 MHz (although the smooth spectrum of FRB 180525 might be caused by an extremely broadband scintle). Thus, if the structure is due to scintillation, it is more readily attributed to a medium external to the Galaxy: either in the interstellar medium of the burst host galaxy, or in some overdense region of intergalactic plasma along the line of sight.

The data are largely inconsistent with the simple prediction that the intensity fluctuations follow an exponential distribution expected of fully modulated scintillation. Table 2 shows that over half of the bursts are inconsistent with fully modulated diffractive scintillation, and none for which there is good discriminating power (high S/N, low $\nu_{\rm dc}$), as embodied in Equation (1).

However, there are three possible ways in which this spectral structure would still be consistent with an interpretation in terms of diffractive scintillation: the number of scintles sampled across the observing band is finite, the structure is spectrally unresolved, or the diffractive scintillation is partially quenched by some physical process. The first explanation is unlikely, as the statistical test used to calculate the confidence values in Table 2 takes into account the finite number of samples. (We note that averaging the data over bandwidths $\sim\nu_{\rm dc}$ should suppress some of the spectral variability, but Figure 4 shows that instead there appears to be a slight excess of observed high fluence events, rather than a deficit, relative to the model.)

Of the second and third possibilities, it is remarkable that the Parkes FRBs, located at a higher average DM, exhibit generally smoother spectra (Thornton et al. 2013; Champion et al. 2016), which is at least consistent with an interpretation in terms of partially quenched scintillation. In contradistinction, two of the lowest DM Parkes bursts (FRBs 150807 and 180309; Ravi et al. 2016; Oslowski et al. 2018) and the lowest DM burst detected by UTMOST (FRB 170827; Farah et al. 2018) do show strong spectral modulation consistent with the ASKAP-CRAFT bursts.

Given this, if the variations are due to diffractive scintillation it behooves us to consider in slightly more detail how an anti-correlation between DM and the amplitude of spectral variability (i.e., partial quenching of the scintillations) may arise. The two mechanisms for this are as follows.

1. DM scales with the scattering measure, causing a commensurate decrease in $\nu_{\rm dc}$. For sufficiently strong scattering $\nu_{\rm dc}$ would fall below our 1 MHz spectral resolution, thus partially quenching the variations. However, the data disfavor this explanation because in most cases the spectral structure is either resolved or marginally resolved. Moreover, suppression of the modulations to $m^2 < 0.1$ would require $\nu_{\rm dc} \lesssim 100$ kHz. This would require $\nu_{\rm dc}$ in these bursts to be considerably lower than the lowest observed at 1.4 GHz with higher-resolution instruments: the narrowest structure at 1.4 GHz has $\nu_{\rm dc} = 100 \pm 50$ kHz (in FRB 150807; Ravi et al. 2016).

2. Angular broadening partially suppresses the amplitude of the spectral variations associated with diffractive scintillation. The Shannon et al. (2018) DM-fluence relation shows that the FRB DMs are related to distance, and the only component of the DM that relates to burst distance is the IGM contribution. A correlation between angular broadening and DM is expected if, as higher DM implies greater distance, there is a greater likelihood of grazing the halo of an intervening galaxy along the light of sight harboring plasma sufficiently dense to produce an appreciable amount of angular broadening. Vedantham & Phinney (2019) discuss the evidence that cold substructure within the baryonic halos of galaxies may easily give rise to the required level of scattering on intergalactic distances (though for one case, Masui et al. 2015, the scattering appears to be more local to the FRB). Scattering from such systems merely requires the burst distances to be sufficient that they intersect the halos of intervening systems, which is a much easier constraint to satisfy than the intersection of a galaxy disk (which typically requires $z \gtrsim 1$).

The optics of angular broadening heavily weights the contribution from scattering material closer to the observer, so the amount of angular broadening need not be directly

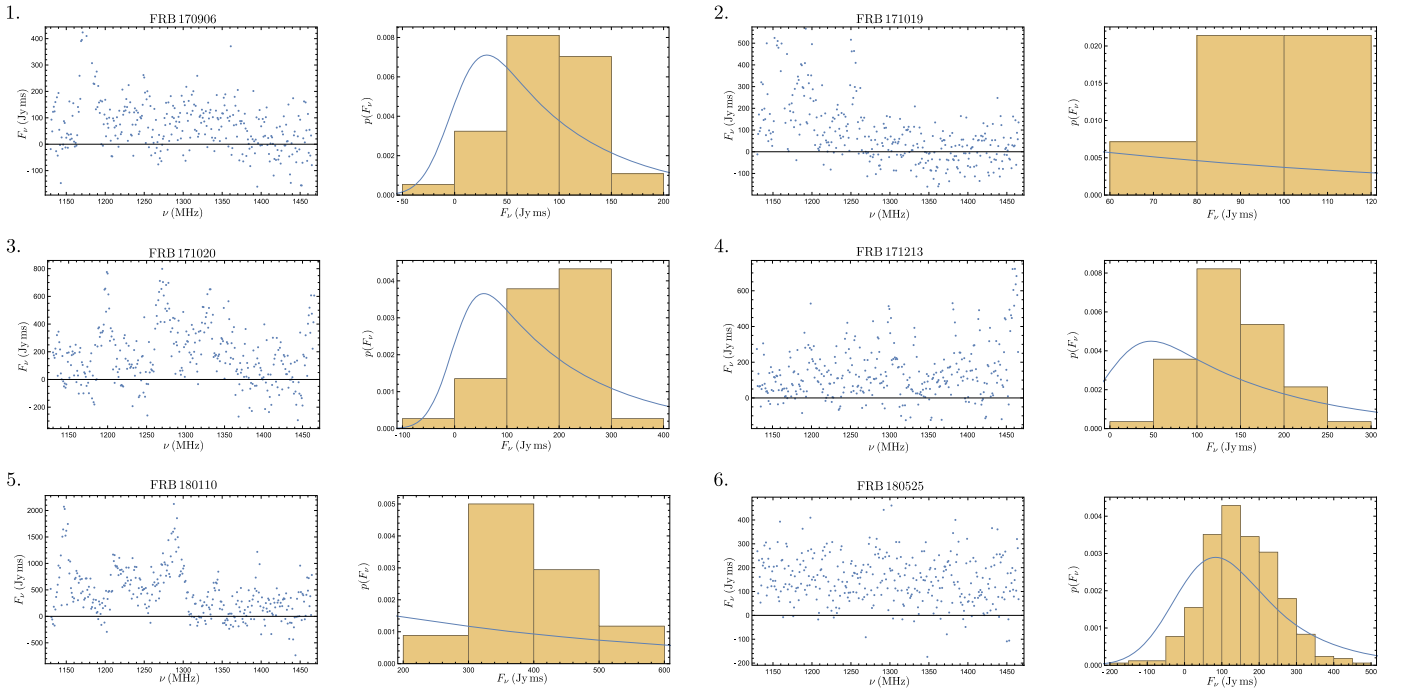

Figure 4. Spectra (left) and the corresponding fluence histograms of all bursts with S/N > 20, after binning to a spectral resolution $\nu_{\rm dc}$ (right). The blue curve shows the predicted probability distribution function for fully modulated diffractive scintillation, as shown in Equation (1).

Table 2
Spectral Properties of Individual FRBs

FRB	S/N[a]	α	$\nu_{\rm dc}$ MHz	Un-normalized Spectrum		Normalized Spectrum	
				m^2 [b]	% Confidence Fits Exp. Distn.	$m^2_{\alpha,\rm corr}$ [b]	% Confidence Fits Exp. Distn.
170107	13.5	−3.5	(3.6)	0.15	3	0.10	5
170416	10.4	−7.5	15	1.0	5	0.80	8
170428	10.2	−2.1	⋯	0 (−0.24)	11	0 (−0.21)	17
170707	11.4	+1.6	1.0	0.49	78	0.58	92
170712	15.4	−4.2	6.9	0.39	0.3	0.33	0.4
170906	25.8	−6.3	9.4	1.7	0.5	1.2	0.4
171003	14.0	+6.6	48	0.48	37	0.75	9
171004	12.4	+2.6	23	0.64	30	0.81	32
171019	23.4	−12	49	2.3	3	1.5	3
171020	28.4	−0.74	8.4	0.86	0.08	0.87	0.09
171116	11.5	+1.7	1.2	0.08	38	0.13	28
171213	28.5	+4.1	5.4	0.66	4×10^{-4}	0.93	1×10^{-3}
171216	8.8	+2.6	2.1	1.06	95	1.05	81
180110	37.4	−4.6	10	0.76	1×10^{-3}	0.64	1×10^{-3}
180119	18.3	−1.1	1.8	0.97	86	0.89	77
180128.2	12.7	+7.3	25	0.76	5	0.82	5
180128.0	15.0	−2.3	12	0.68	0.6	0.69	1
180130	11.5	+0.49	0.4	0.30	55	0.41	50
180131	14.4	−2.4	1.3	0.33	1	0.32	1
180212	17.7	−3.7	2.8	0.60	0.3	0.51	0.2
180315	9.3	−0.63	5.9	0.08	11	0.05	8
180324	9.0	+0.85	1.3	0.72	93	0.84	96
180525	31.2	−1.3	0.36	0.06	2×10^{-6}	0.06	3×10^{-6}

Notes.
[a] This post-detection S/N differs slightly from the detection S/N reported in Shannon et al. (2018) and, for FRBs 171216 and 180525, is the result of co-addition of data from two adjacent beams.
[b] The measured value of the autocovariance at $\Delta\nu = 1$ MHz is negative for FRB 170428, so we take $m^2 = m^2_{\alpha,\rm corr} = 0$ for this burst. However, we note that this could instead indicate spectral modulation with $\nu_{\rm dc} \ll 1$ MHz, in which case the data could be more consistent with a diffractive scintillation interpretation at better than the 11%–17% level indicated for this burst.

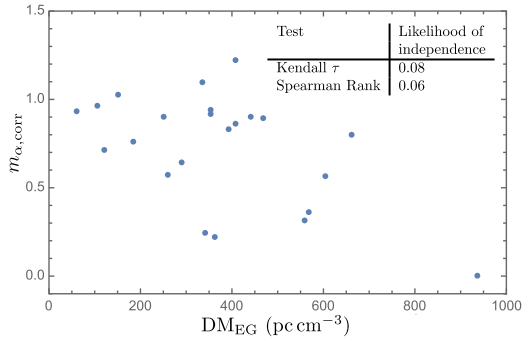

Figure 5. Distribution of $m_{\alpha,\mathrm{corr}}$ against burst $\mathrm{DM_{EG}}$.

coupled with temporal smearing, which favors the contribution of material closer to midway along the ray path. Thus the absence of temporal smearing (e.g., in the DM = 2596 pc cm^{-3} FRB 160102; Bhandari et al. 2018) does not imply an absence of scatter broadening and, conversely, the presence of temporal smearing (e.g., in FRB 180110) does not necessarily imply detectable angular broadening.

We examined the data for evidence of any anti-correlation between the DM and the amplitude of the spectral modulation, and found weak evidence for this, thus favoring its interpretation as a propagation effect. Specifically, we examined the likelihood of the hypothesis that $\mathrm{DM_{EG}}$ and $m_{\alpha,\mathrm{corr}}$ are independent in the ASKAP-CRAFT sample. The Spearman rank test and Kendall tau tests return likelihoods of 6% and 8%, with correlation coefficients of -0.4 and -0.3, respectively. A plot of the DM-modulation relation is shown in Figure 5.

In summary, although it is not possible to reach a definitive conclusion on the origin of the spectral structure, circumstantial evidence from UTMOST and Parkes FRBs, and weak evidence for a DM-modulation index relation, favor its interpretation in terms of diffractive scintillation from a medium external to the Milky Way.

5. Discussion

The mean spectral index measured for the bright FRB population, $\alpha = -1.5^{+0.2}_{-0.3}$, is consistent with the range $\alpha = -1.4$ to -1.6 typically derived for the slow and millisecond pulsar populations (Bates et al. 2013; Jankowski et al. 2018), but apparently at variance with the spectral index of giant pulses and magnetars. An index of $\alpha = -2.6$ is derived from the giant pulses from the well-studied Crab pulsar between 0.7 and 3.1 GHz (Meyers et al. 2017), while the range of radio spectral indices typical of magnetar emission is flat, with $\alpha > -0.5$ (Camilo et al. 2007, 2008; Levin et al. 2010; Eatough et al. 2013). Although it is premature to draw conclusions on the mechanism responsible for the ultraluminous emission from FRBs, the similarity in spectral indices hints at an association with spin-down-powered pulsar emission. It might be argued that the large range of spectral indices measured between bursts precludes a physical interpretation of the mean spectral index, but this will not be the case if diffractive scintillation is the primary cause of spectral variability, where an average over a sufficiently large ensemble of independent scintles (even along different lines of sight) would converge to a statistically meaningful quantity.

The steep spectral index of FRB emission implies that the location of the low-frequency turnover is crucial in understanding the total radio energy output. The 200 MHz MWA non-detections of several bright FRBs in the sample analyzed here sets limits on the total radiative output below 1.5 GHz to <18 times that observed in the ASKAP band (Sokolowsi et al. 2018). However, the reported CHIME detections of some FRBs above 400 MHz (Amiri et al. 2019) appear to bracket the range of any spectral turnover, at least from the standpoint of average spectral occupancy in the population.

The steepness of bright FRB emission underlines the importance of the k-correction in the determination of burst luminosities and energies (see the discussion in Macquart & Ekers 2018). For a burst at luminosity distance $D_L(z)$ the fluence and intrinsic energy density, F_ν are related by $F_\nu = (1+z)^{2+\alpha} F_\nu / (4\pi D_L^2(z))$. Thus the fluence of a $z = 1$ burst is a factor of 2.8 lower relative to one of same energy density but a flat spectrum.

A pervasive feature of the ASKAP-CRAFT FRB spectra is their patchiness. There is a large degree of spectral variation between individual bursts, resembling the spectrally erratic emission from the repeating FRB 121102 (Scholz et al. 2016; Spitler et al. 2016).

The origin of this spectral structure in the bright FRB population remains inconclusive, and it may yet be an intrinsic property of the bursts. Nonetheless, it appears most probable that at least part of the structure is caused by diffractive scintillation, and if the inverse relation between the amount of spectral structure and the DM weakly favored by the ASKAP-CRAFT data should be confirmed, it may be caused by the angular broadening in the halos of intervening galaxies embedded in the IGM.

The generally smoother spectral structure observed in Parkes FRBs lends credence to the hypothesis that the fine spectral structure is indeed a propagation effect. Incorporation of spectral information from the full Parkes FRB sample would provide a far stronger statistical test for the presence of a DM-spectral modulation relation.

The Australian SKA Pathfinder is part of the Australia Telescope National Facility which is managed by CSIRO. Operation of ASKAP is funded by the Australian Government with support from the National Collaborative Research Infrastructure Strategy. ASKAP uses the resources of the Pawsey Supercomputing Centre. Establishment of ASKAP, the Murchison Radio-astronomy Observatory, and the Pawsey Supercomputing Centre are initiatives of the Australian Government, with support from the Government of Western Australia and the Science and Industry Endowment Fund. We acknowledge the Wajarri Yamatji people as the traditional owners of the Observatory site. J.P.M., R.M.S., and K.B. acknowledge funding through Australian Research Council grant DP180100857. R.M.S. also acknowledges support through Australian Research Council (ARC) grants FL150100148 and CE170100004.

ORCID iDs

J.-P. Macquart https://orcid.org/0000-0001-6763-8234
R. M. Shannon https://orcid.org/0000-0002-7285-6348
K. W. Bannister https://orcid.org/0000-0003-2149-0363
C. W. James https://orcid.org/0000-0002-6437-6176
R. D. Ekers https://orcid.org/0000-0002-3532-9928

References

Amiri, M., Bandura, K., Bhardwaj, M., et al. 2019, Natur, doi:10.1038/s41586-018-0867-7
Bannister, K. W., Shannon, R. M., Macquart, J.-P., et al. 2017, ApJL, 841, L12
Bannister, K. W., Stevens, J., Tuntsov, A. V., et al. 2016, Sci, 351, 354
Bates, S. D., Lorimer, D. R., & Verbiest, J. P. W. 2013, MNRAS, 431, 1352
Bhandari, S., Keane, E. F., Barr, E. D., et al. 2018, MNRAS, 475, 1427
Bhat, N. D. R., Tremblay, S. E., Kirsten, F., et al. 2018, ApJS, 238, 1
Camilo, F., Ransom, S. M., Peñalver, J., et al. 2007, ApJ, 669, 561
Camilo, F., Reynolds, J., Johnston, S., Halpern, J. P., & Ransom, S. M. 2008, ApJ, 679, 681
Champion, D. J., Petroff, E., Kramer, M., et al. 2016, MNRAS, 460, L30
Cordes, J. M., & Lazio, T. J. W. 2002, arXiv:astro-ph/0207156
Cordes, J. M., & Wasserman, I. 2016, MNRAS, 457, 232
Cordes, J. M., Wasserman, I., Hessels, J. W. T., et al. 2017, ApJ, 842, 35
Dolag, K., Gaensler, B. M., Beck, A. M., & Beck, M. C. 2015, MNRAS, 451, 4277
Eatough, R., Karuppusamy, R., Champion, D., et al. 2013, ATel, 5058, 1
Ellis, G. R. A. 1969, AuJPh, 22, 177
Farah, W., Flynn, C., Bailes, M., et al. 2018, MNRAS, 478, 1209
Hankins, T. H., & Eilek, J. A. 2007, ApJ, 670, 693
Jankowski, F., van Straten, W., Keane, E. F., et al. 2018, MNRAS, 473, 4436
Levin, L., Bailes, M., Bates, S., et al. 2010, ApJ, 721, L33
Lorimer, D. R., Bailes, M., McLaughlin, M. A., Narkevic, D. J., & Crawford, F. 2007, Sci, 318, 777
Macquart, J.-P., Bailes, M., Bhat, N. D. R., et al. 2010, PASA, 27, 272
Macquart, J. P., & Ekers, R. 2018, MNRAS, 480, 4211
Masui, K., Lin, H.-H., Sievers, J., et al. 2015, Natur, 528, 523
McConnell, D., Allison, J. R., Bannister, K., et al. 2016, PASA, 33, e042
Melrose, D. B. 2017, RvMPP, 1, 5
Melrose, D. B., & Yuen, R. 2016, JPlPh, 82, 635820202
Mercier, R. P. 1962, MPCPS, 58, 382
Metzger, B. D., Berger, E., & Margalit, B. 2017, ApJ, 841, 14
Meyers, B. W., Tremblay, S. E., Bhat, N. D. R., et al. 2017, ApJ, 851, 20
Oslowski, S., Shannon, R. M., Jameson, A., et al. 2018, ATel, 11385, 1
Petroff, E., Barr, E. D., Jameson, A., et al. 2016, PASA, 33, e045
Ravi, V., Shannon, R. M., Bailes, M., et al. 2016, Sci, 354, 1249
Salpeter, E. E. 1967, ApJ, 147, 433
Scholz, P., Spitler, L. G., Hessels, J. W. T., et al. 2016, ApJ, 833, 177
Shannon, R. M., Macquart, J. P., Bannister, K. W., et al. 2018, Natur, 562, 386
Sokolowsi, M., Bhat, N., & Macquart, J.-P. 2018, ApJL, 867, L12
Spitler, L. G., Scholz, P., Hessels, J. W. T., et al. 2016, Natur, 531, 202
Tendulkar, S. P., Bassa, C. G., Cordes, J. M., et al. 2017, ApJL, 834, L7
Thornton, D., Stappers, B., Bailes, M., et al. 2013, Sci, 341, 53
Vachaspati, T. 2008, PhRvL, 101, 141301
Vedantham, H. K., & Phinney, E. S. 2019, MNRAS, 483, 971